

Article

Transfer Matrix Method for the Analysis of Multiple Natural Frequencies

Jinghong Wang ^{1,2}, Xiaoting Rui ^{1,2}, Bin He ^{1,2,*}, Xun Wang ^{1,2}, Jianshu Zhang ^{1,2} and Kai Xie ^{1,2}

¹ National Key Laboratory of Complex Multibody System Dynamics, Nanjing University of Science and Technology, Nanjing 210094, China; 317108010146@njust.edu.cn (J.W.); ruixt@njust.edu.cn (X.R.); xunwang@njust.edu.cn (X.W.); jszhang@njust.edu.cn (J.Z.)

² Institute of Launch Dynamics, Nanjing University of Science and Technology, Nanjing 210094, China

* Correspondence: hebin@njust.edu.cn

Abstract: Multiple natural frequencies may be encountered when analyzing the essential natural vibration of a symmetric mechanical system or sub-structure system or a system with special parameters. The transfer matrix method (TMM) is a useful tool for analyzing the natural vibration characteristics of mechanical or structural systems. It derives a nonlinear eigen-problem (NEP) in general, even a transcendental eigen-problem. This investigation addresses the NEP in TMM and proposes a novel method, called the determinant-differentiation-based method, for calculating multiple natural frequencies and determining their multiplicities. Firstly, the characteristic determinant is differentiated with respect to frequency, transforming the even multiple natural frequencies into the odd multiple zeros of the differentiation of the characteristic determinant. The odd multiple zeros of the first derivative of the characteristic determinant and the odd multiple natural frequencies can be obtained using the bisection method. Among the odd multiple zeros, the even multiple natural frequencies are picked out by the proposed judgment criteria. Then, the natural frequency multiplicities are determined by the higher-order derivatives of the characteristic determinant. Finally, several numerical simulations including the multiple natural frequencies show that the proposed method can effectively calculate the multiple natural frequencies and determine their multiplicities.

Keywords: linear vibration; multiple natural frequencies; nonlinear eigen-problem; transfer matrix method; determinant derivatives; multibody system transfer matrix method

MSC: 70J10



Citation: Wang, J.; Rui, X.; He, B.; Wang, X.; Zhang, J.; Xie, K. Transfer Matrix Method for the Analysis of Multiple Natural Frequencies. *Mathematics* **2024**, *12*, 1413. <https://doi.org/10.3390/math12091413>

Academic Editor: Arnulfo Luévanos-Rojas

Received: 12 March 2024

Revised: 25 April 2024

Accepted: 27 April 2024

Published: 6 May 2024



Copyright: © 2024 by the authors. Licensee MDPI, Basel, Switzerland. This article is an open access article distributed under the terms and conditions of the Creative Commons Attribution (CC BY) license (<https://creativecommons.org/licenses/by/4.0/>).

1. Introduction

Natural vibration analysis is essential for dynamic design and manufacturing of mechanical systems [1,2]. In the process of the natural vibration analysis, the multiple eigenvalues, i.e., the multiple natural frequencies for undamped systems and the multiple complex eigenvalues for damped systems, may be encountered if a mechanical system or a sub-structure system is symmetrical and its boundary conditions are also symmetric, or the system parameters are specially chosen. Determination for the frequency multiplicity is essential for these systems such as the reduced-order model [3], the optimization design [4,5], and so on.

Besides the widely used finite element method (FEM) [6], the transfer matrix method (TMM) is also a useful tool for analyzing the natural vibration characteristics of a mechanical system, which fully utilizes both the analytical and numerical approximation solutions of the mathematical models for individual elements. Especially for chain mechanical systems, the method only involves the low-order matrices. It has been applied to many applications [7–13] including wave propagation of panels [7], beam structures [8], rotor-bearing systems [9–11], vibration and acoustics of pipes [12,13], etc. Rui et al. [14]

greatly improved the classical TMM of vibration mechanics and developed the multi-body system transfer matrix method (MSTMM), including vibration analysis, frequency response analysis and transient analysis for mechanical systems with linear vibration and large motion. It was reported that the MSTMM already has approximately 150 different applications [15], including but not limited to engineering software [15], a fly-cutting machine-tool [2], helicopter-driven system [16], rotating machinery [17], and so on.

For analyzing the vibration characteristic of the undamped mechanical systems, both the TMM and MSTMM derive the following eigen-equation [14]:

$$\bar{\mathbf{U}}(\omega)\bar{\mathbf{Z}} = \mathbf{0} \quad (1)$$

where ω denotes the natural frequency, $\bar{\mathbf{Z}}$ denotes the reduced state vector that summarizes the unknown modal displacements and forces at the system boundary, and the coefficient matrix $\bar{\mathbf{U}}$ is derived from the system overall transfer matrix according to the system boundary conditions. Solving this eigen-equation enables the natural frequencies ω and reduced state vector $\bar{\mathbf{Z}}$ to be obtained. Here, we address the multiple natural frequencies and determine their multiplicities by solving the above eigen-equation.

Different from the general eigen-problem in the FEM [6], the eigen-equation, as shown in Equation (1), always contains the nonlinear functions, even transcendental functions, of the natural frequencies. Thus, solving this eigen-equation is called the nonlinear eigen-problem (NEP), even in cases of transcendental eigen-problems mathematically. The NEP is reported as a challenge for the modern eigen-problem and includes the quadratic eigen-problem, the polynomial eigen-problem, the rational eigen-problem and the transcendental eigen-problem. Generally, the direct way to solve the quadratic eigen-problem and polynomial eigen-problem is to adopt the linearization method, resulting in the general eigen-problem with the first or second type of companion matrices [18,19]. Since the linearization method increases the matrix order, it is the choice if the properties are unclear. In addition, the commonly used methods include the Newton-type method [18,20–23] and iterative projection method [24–27]. It was reported that no classical methods can work perfectly for these NEP, and only the methods dealing with the specific structures provide sufficiently accurate eigenvalues [18,27]. However, the NEP derived in TMM, as well as MSTMM, represented by Equation (1), has no specific properties. It may be a polynomial eigen-problem, rational eigen-problem, or transcendental eigen-problem, even their combination, which depends on the types of the utilized elements when modeling the mechanical or structural systems.

To the best of the author's knowledge, only a few techniques exploiting the model characteristics have been developed for NEP, especially the transcendental eigen-problem, among which the famous Wittrick–Williams algorithm [28] is notable. This algorithm can be regarded as an extension of the Sturm sequences method, and the latter is commonly used for solving the general eigen-problem [6]. The Wittrick–Williams algorithm precisely counts the number of the natural frequencies below a given trial frequency by utilizing the residual dynamic stiffness matrix [28,29]. It has been applied in various fields including structural dynamics analysis [29–33], linear buckling analysis [34,35], etc. Several improvements and extensions have been proposed to enhance its efficiency [36] and capabilities [32,33]. However, due to the symmetry assumptions of the dynamic stiffness matrix, both the Wittrick–Williams algorithm and its enhancements are not directly applicable for solving the resulting NEP in both TMM and MSTMM, where the coefficient matrix of the derived eigen-equation is asymmetric.

Another widely used strategy for solving NEP in both the TMM and MSTMM is to transform them into the root-finding problems of the characteristic equation, i.e., the algebraic equation expressed by the determinant of the coefficient matrix of the eigen-equation shown as Equation (1). This allows solving NEP to be equivalent to solving the resulting nonlinear algebraic equation [14,37–39] with respect to the natural frequency ω . This strategy is feasible because the TMM, as well as MSTMM, only involves the low-order matrices. Murthy [37] employed the Newton iteration method to solve the

derived determinant equation from NEP for the flutter frequency in aeroelasticity. Xue [38] proposed a method combining the dynamic finite element with the Riccati TMM for solving the rational eigen-problem. The Muller iteration method, Brent method, Newton iteration and quasi-Newton method [40] are suitable for finding a certain root, but their local convergence means it requires guessing a proper initial value to ensure the local convergence when searching for a certain root. However, a proper guess for a complex mechanical or structural model is usually difficult. Moreover, when searching for the next natural frequency within the trial frequency, the obtained natural frequencies should be effectively stepped over during the subsequent iterations. Since the essential eigenvalues are of the first several orders, they cannot directly meet the specific requirements for solving the multi-root problem. Therefore, in TMM, the bisection method is widely applied to find all the natural frequencies below a trial frequency [14] for its robustness. It is foolproof for searching the odd multiple natural frequencies as long as the interval resolution can identify the densest frequencies. However, the original bisection method, through identifying the sign changes in function values on both sides, can only find the odd multiple natural frequencies, including the distinct natural frequencies, rather than the even multiple natural frequencies. Given these, Bestle et al. [39] proposed an extreme-based method called the “recursive eigenvalue searching algorithm” (RESA) to solve the NEP in MSTMM. This method transforms the root-finding problem into a minimization problem. In the RESA, a minimum point may be incorrectly identified as a natural frequency of the system if it is a non-zero minimum of the absolute value of the characteristic determinant. Moreover, no methods are available for determining the multiplicities of the natural frequencies in both MSTMM and TMM.

Therefore, when using TMM, as well as MSTMM, it is crucial to develop a more stable and reliable method to resolve even multiple natural frequencies and determine the multiplicities of all the natural frequencies.

This paper addresses the calculation of natural frequencies and determination of their multiplicities of mechanical systems. In this paper, Section 2 presents a brief overview of TMM, and then Section 3 illustrates a novel method, named the determinant-differentiation-based method, to calculate the multiple natural frequencies for the derived NEP. Firstly, the even multiple natural frequencies are calculated by transforming them into zeros of the first derivative of the characteristic determinant. Then, judgment criteria are proposed to identify and select the even multiple natural frequencies from the zeros of this first derivative. The remaining odd multiple natural frequencies are directly obtained by finding the zeros of the characteristic determinant using the bisection method. Subsequently, we utilize the higher-order derivatives of the characteristic determinant with respect to frequency to determine the multiplicities of all the natural frequencies. Finally, Section 4 presents several numerical simulations with multiple natural frequencies to validate the proposed method for calculating these frequencies and determining their multiplicities. Among them, the basic ideas, the judgment criteria, and the method to determine the multiplicities are original. They are outlined in Sections 3.1, 3.3 and 3.4, respectively. Section 3.2 mainly deduces an alternative to Jacobi’s formula to obtain the derivative without matrix inversion for the fact that the coefficient matrix \bar{U} near the natural frequency is almost singular.

2. Principle of Transfer Matrix Method

In TMM [14], for a spatially vibratory element, the state vector of each connection point may be defined as, i.e.,

$$\mathbf{Z} = [\mathbf{R}^T \quad \Theta^T \quad \mathbf{M}^T \quad \mathbf{Q}^T]^T \quad (2)$$

where R , Θ , M and Q denote the modal translational displacements, rotational angles, forces and moments, respectively. Their array forms in three axis directions of the element's inertial frame can be given as follows:

$$R = \begin{bmatrix} X \\ Y \\ Z \end{bmatrix}, \Theta = \begin{bmatrix} \Theta_X \\ \Theta_Y \\ \Theta_Z \end{bmatrix}, M = \begin{bmatrix} M_X \\ M_Y \\ M_Z \end{bmatrix}, Q = \begin{bmatrix} Q_X \\ Q_Y \\ Q_Z \end{bmatrix} \tag{3}$$

The state vectors of connection points of each element are divided into input I and output O . For the element i with a single input and single output, the relationships between its state vectors can be expressed as the transfer equation [14]:

$$Z_{i,O} = U_i Z_{i,I} \tag{4}$$

where U_i is the element transfer matrix. For any branch element i with multiple inputs and a single output, the relationships among its state vectors are expressed as follows [14]:

$$Z_{i,O} = \sum_{k=1}^N U_{i,I_k} Z_{i,I_k} \tag{5}$$

where N denotes the number of inputs of this branch element, I_k ($k = 1, 2, \dots, N$) denotes the k -th input, and U_{i,I_k} denotes the element transfer matrix from input I_k to output O . Additionally, the consistency equations should be supplemented due to the state vector dependency of its inputs. For a rigid body with multiple inputs and a single output, its consistency equations can be expressed as follows [14,15]:

$$H_{i,I_1} Z_{i,I_1} + H_{i,I_N} Z_{i,I_N} = 0, k = 2, 3, \dots, N \tag{6}$$

where H_{i,I_k} ($k = 1, 2, \dots, N$) denotes the coefficient matrix corresponding to the k -th input of branch element i . For a flexible body, the consistency equations can be found in Ref. [2].

The state vectors of the intermediate connection points within the system can be recursively eliminated from the system inputs to the system output, and the system overall transfer equation is finally derived [14]:

$$U_{all} Z_{all} = 0 \tag{7}$$

where the boundary state vector of the system Z_{all} is composed of the state vectors of the system boundary, while the coefficient matrix U_{all} of Equation (7) is called the overall transfer matrix. Excluding the corresponding columns and rows of U_{all} according to the zeros in Z_{all} , the final eigen-equation is deduced as shown in Equation (1). The nontrivial solution \bar{Z} of Equation (1) requires a singular coefficient matrix, leading to the following characteristic equation:

$$\Delta(\omega) := \det U = 0 \tag{8}$$

In general, Equation (8) is solved to obtain the odd multiple natural frequencies, especially the distinct natural frequencies, by using the methods such as the bisection method [14], RESA [39], and so on. In the next section, a stable and reliable method will be developed to resolve multiple natural frequencies, including those with even multiplicities, and the multiplicities of all the natural frequencies will be determined.

3. Multiple Natural Frequency Analysis

Unless otherwise noted, the first and k -th order derivatives of (\cdot) with respect to ω can be expressed as follows:

$$(\bullet)' = \frac{d(\bullet)}{d\omega}, (\bullet)^{(k)} = \frac{d^k(\bullet)}{d\omega^k} \tag{9}$$

3.1. Basic Ideas

If a mechanical system has the multiple natural frequencies, its characteristic equation. Equation (8) will have multiple roots. According to the definition of multiple roots in algebraic equations [41], for the infinitely differentiable function $\Delta(\omega)$ with respect to the single variable ω , ω^* is an m -multiple zero of $\Delta(\omega)$ if and only if the following condition is satisfied:

$$\Delta(\omega^*) = \Delta'(\omega^*) = \dots = \Delta^{(m-1)}(\omega^*) = 0 \wedge \Delta^{(m)}(\omega^*) \neq 0 \tag{10}$$

This equation implies that ω^* is the $m - 1$ multiple zero of $\Delta'(\omega)$. Thus, it can be found that every even multiple zero of Δ is the odd multiple zero of Δ' and is used to transfer the even multiple zero of Δ into the odd multiple zero of Δ' . Moreover, an m -multiple zero of $\Delta(\omega)$ is also the zero of the k -th derivative $\Delta^{(k)}(\omega)$ if $k < m$, while it is not the zero of $\Delta^{(k)}(\omega)$ if $k \geq m$.

3.2. First Derivative of the Characteristic Determinant

Based on the above basic idea, the even multiple natural frequencies of the system can be obtained by directly using the bisection method to solve the following nonlinear algebraic equation for the odd multiple roots:

$$\Delta'(\omega) = 0 \tag{11}$$

The first derivative of the determinant Δ with respect to the natural frequency ω can be obtained by utilizing Jacobi's formula [19]:

$$\Delta'(\omega) = \Delta(\omega) \text{tr} \begin{pmatrix} - & - & - \\ \mathbf{U} & \mathbf{U} & \end{pmatrix} \tag{12}$$

where $\text{tr}(\cdot)$ denotes the trace of matrix (\cdot) . Due to the singularity near the exact solution ω^* , it is necessary to avoid the matrix inversion. Consider the following equation:

$$\mathbf{U}^{-1} = \frac{1}{\Delta(\omega)} \text{adj} \mathbf{U} \tag{13}$$

where $\text{adj}(\cdot)$ denotes the adjacent matrix of (\cdot) , Equation (12) can be expressed as follows:

$$\Delta'(\omega) = \sum_{k=1}^N \sum_{j=1}^N \left\{ \left(\text{adj} \mathbf{U} \right) \right\}_{kj} \left\{ \mathbf{U} \right\}_{jk} \tag{14}$$

where $\{\cdot\}_{ik}$ denote the component in the i -th row and the k -th column of matrix (\cdot) .

The definition of the adjacent matrix yields the following:

$$\begin{aligned} & \sum_{j=1}^N \left\{ \text{adj} \left(\mathbf{U} \right) \right\}_{kj} \left\{ \mathbf{U} \right\}_{jk} \\ &= \det \left[\begin{array}{ccccccc} \text{col}_1 \mathbf{U} & \dots & \text{col}_{k-1} \mathbf{U} & \text{col}_k \mathbf{U} & \text{col}_{k+1} \mathbf{U} & \dots & \text{col}_N \mathbf{U} \end{array} \right] \end{aligned} \tag{15}$$

where $\text{col}_k(\cdot)$ denotes the components in the k -th column of matrix (\cdot) .

Therefore, the equivalent formula of $\Delta'(\omega)$ can be derived from Equations (14) and (15) as follows:

$$\Delta'(\omega) = \sum_{k=1}^N \det \left[\begin{array}{ccccccc} \text{col}_1 \mathbf{U} & \dots & \text{col}_{k-1} \mathbf{U} & \text{col}_k \mathbf{U} & \text{col}_{k+1} \mathbf{U} & \dots & \text{col}_N \mathbf{U} \end{array} \right] \tag{16}$$

Although Equation (16) requires more computational time than Equation (12) due to computing N determinants, the MSTMM only involves very low-order matrices; thus, using

Equation (16) instead of Equation (12) to avoid the matrix inversion of \bar{U} near the exact solution ω^* is feasible. Therefore, according to Equation (16), the characteristic determinant derivative can be deduced by calculating \bar{U} and its derivative \bar{U}' .

Thus, by utilizing the bisection method with scanning intervals and identifying the sign changes in Δ' at the two sides of each rooted interval, the zeros of Equation (11) can encompass the even multiple natural frequencies of the system, where the first derivative of the characteristic determinant are calculated using Equation (16).

3.3. Judgment Criteria for Picking out the Even Multiple Natural Frequencies

Since Equation (11) only gives the odd multiple zeros of $\Delta'(\omega)$, i.e., the stagnation points of the differentiable function $\Delta(\omega)$, it is crucial to introduce practical judgment criteria for picking out part of the zeros of $\Delta'(\omega)$, which are the zeros of $\Delta(\omega)$. Such judgment criteria will be proposed in this section and thereby pick out even multiple natural frequencies.

To clearly illustrate the fact that zeros of $\Delta'(\omega)$ may not be the zeros of $\Delta(\omega)$, a spatially cantilever beam, as illustrated in Figure 1, is selected as an example.

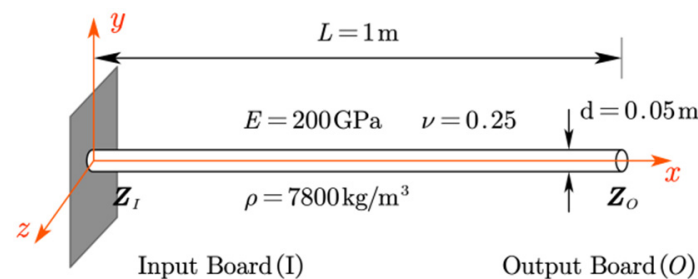


Figure 1. A spatial cantilever beam with multiple frequencies.

This beam is modeled as a uniform Euler beam with a circular cross-section, which has a diameter of 0.05 m, a Young’s modulus of 200 GPa, a density of 7800 kg/m³, and a length of 1 m. This structural system is symmetric and thereby has multiple natural frequencies related to the flexure vibration modes. The transfer matrix of the spatially vibratory Euler beam can be found in Ref. [14]. According to the fixed-free boundary condition, the characteristic determinant can be derived, whether using MSTMM and TMM, using the following equation:

$$\Delta(\omega) = \frac{1}{4}(1 + \cos \lambda L \cos \lambda L)^2 \cos \beta L \cos \gamma L \tag{17}$$

where $\lambda = (\bar{m}\omega^2/EI)^{1/4}$, $\beta = \sqrt{\bar{m}\omega^2/EA}$ and $\gamma = \omega\sqrt{E/[2\rho(v+1)]}$. Here, \bar{m} , EI and EA represent the line mass density, bending stiffness and tensile stiffness. Equation (17) gives the double multiple frequencies that satisfy $1 + \cos\lambda L\cos\lambda L = 0$ and the distinct frequencies that satisfy $\cos\beta L = 0$ or $\cos\gamma L = 0$. $\Delta(\omega)$ and its derivative are plotted in Figure 2, where they are scaled using the following continuous function: $f \mapsto \text{sgn}(f)\log_{10}(1 + |f|)$. Here, $f = \Delta(\omega)$ or $\Delta'(\omega)$. In Figure 2, the markers “ ∇ ” and “ Δ ” represent the odd multiple natural frequencies and even multiple natural frequencies, respectively, while “ \circ ” represents the numerical values that are the zeros of $\Delta'(\omega)$ but not the zeros of $\Delta(\omega)$. The odd multiple natural frequencies are not the zeros of $\Delta'(\omega)$ because of their multiplicities of 1, which are the tensile natural frequencies and torsional natural frequencies and can be obtained by directly solving Equation (17) using the bisection method.

In Figure 2, we can see that the characteristic determinant $\Delta(\omega)$ has a sign change on both sides of the odd multiple natural frequencies but no sign change on both sides of the even multiple natural frequencies. Therefore, the even multiple natural frequencies, i.e., the bending natural frequencies, cannot be obtained by solving Equation (8) with the bisection method due to there being no sign changes for $\Delta(\omega)$ at two sides of the intervals

containing the even multiple zeros. Fortunately, they are also the odd multiple roots of $\Delta'(\omega)$, which can be obtained by solving Equation (11) using the bisection method.

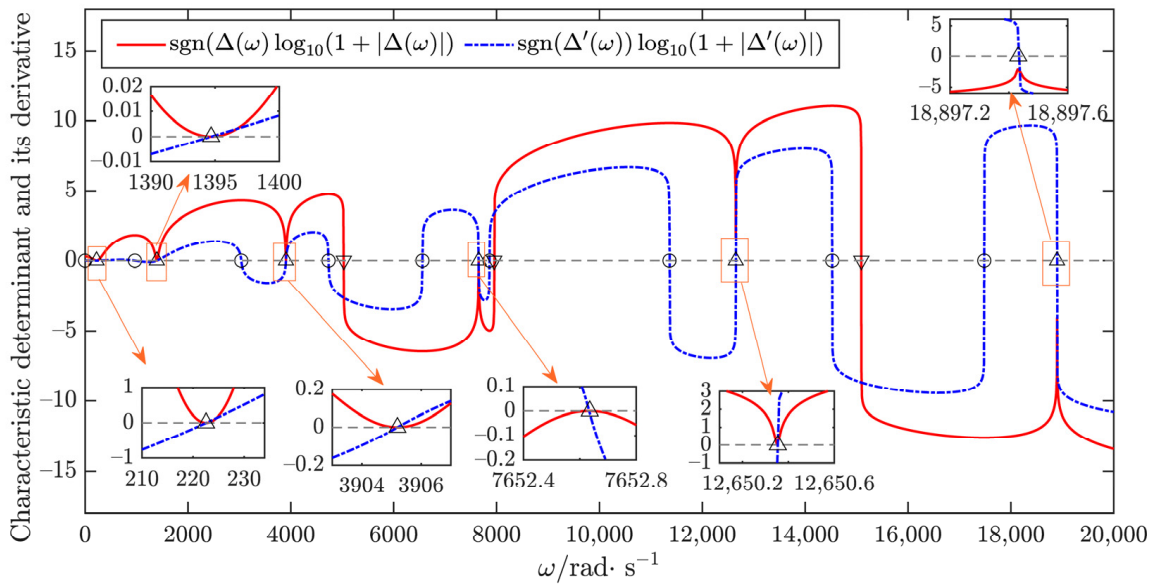


Figure 2. Characteristic determinant and its derivative of spatial chain system composed of one straight uniform Euler beam (“○”, “▽”, and “△” denote the non-zeros of the determinant, odd multiple frequencies, and even multiple frequencies).

Obviously, several zeros of $\Delta'(\omega)$, which are marked by “○” in Figure 2, are not the zeros of $\Delta(\omega)$, but the even multiple natural frequencies are both the zeros of $\Delta(\omega)$ and $\Delta'(\omega)$. The zeros of $\Delta'(\omega)$ not equal to the natural frequencies should be effectively excluded.

On the other hand, due to the inherent floating-point errors of computers, Equation (8) cannot be perfectly satisfied for even multiple roots, although it can be satisfied with the required absolute error. The numerical value of $\Delta(\omega)$ may be large or small near the exact natural frequency ω^* . For example, further details for $\Delta(\omega)$ near the even multiple natural frequencies of this structural system are presented in Figure 3a–f.

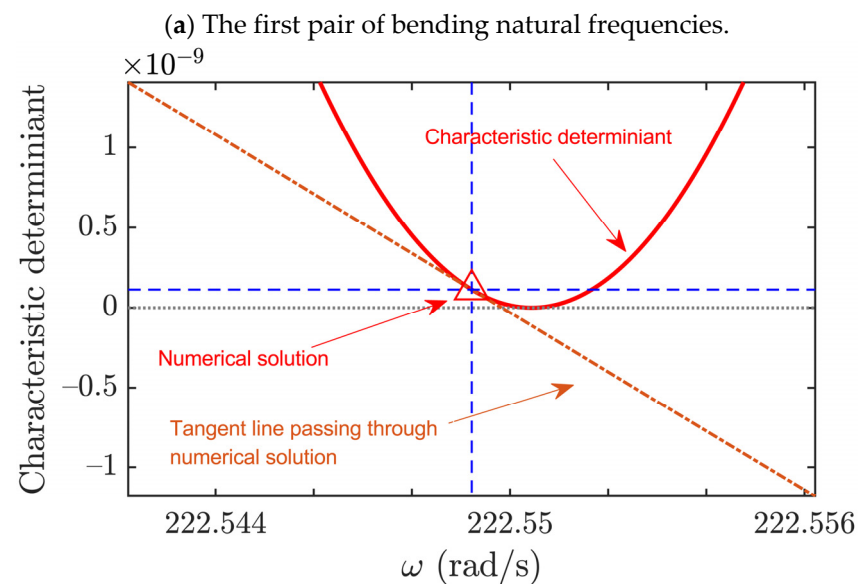


Figure 3. Cont.

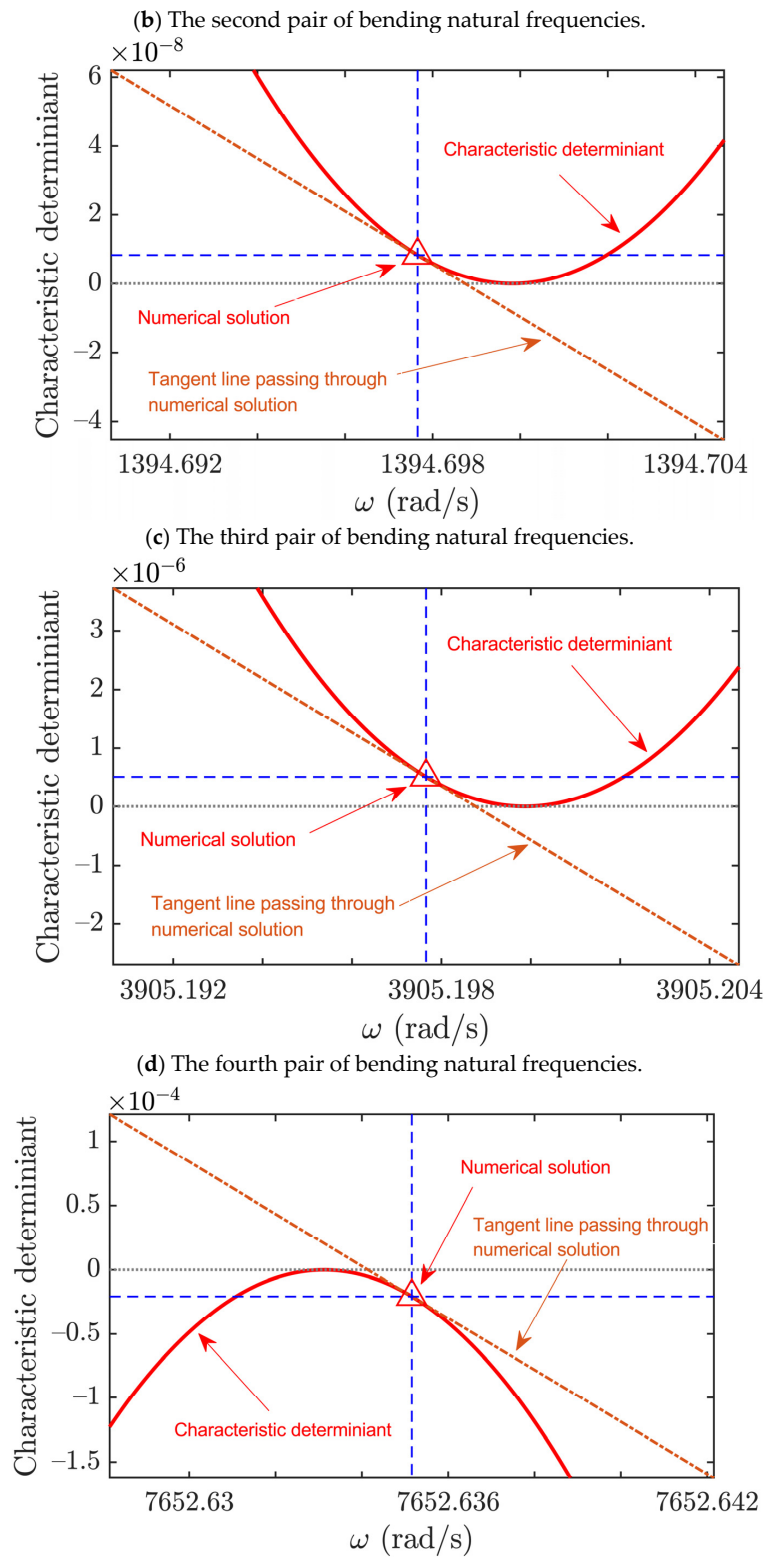
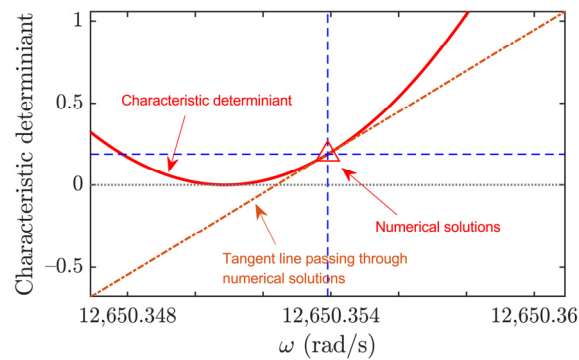


Figure 3. Cont.

(e) The fifth pair of bending natural frequencies.



(f) The sixth pair of bending natural frequencies.

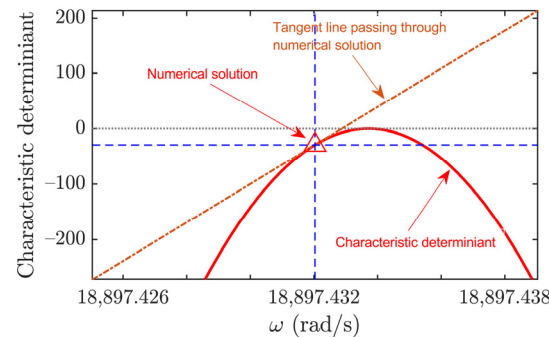


Figure 3. Numerical values of $\Delta(\omega)$ near the first 6 pairs of even natural frequencies (bending modes).

In Figure 3a–f, numerical solutions of these even multiple natural frequencies are obtained within the absolute error of 0.01 rad/s and marked by “ Δ ” in red, which are all the bending natural frequencies with a multiplicity of 2. The tangents passing through the numerical solutions are plotted with orange dash-dotted lines. From Figure 3, it can be seen that the values of $\Delta(\omega)$ in the numerical solutions are not zero and may be numerically small, as shown in Figure 3a–d, or numerically large, as shown in Figure 3e,f.

Thus, the upper bounds of the determinant $\Delta(\omega)$ near the natural frequencies, which are used to exclude the non-zeros of Equation (8) among the roots of Equation (11) to pick out the even multiple natural frequencies, cannot be given artificially as a fixed value. This upper bounds should be given adaptively based on the change rates of $\Delta(\omega)$. Therefore, it is crucial to introduce criteria to effectively exclude the zeros that are not equal to the natural frequencies within the absolute error among the odd multiple zeros of $\Delta'(\omega)$.

Let $E(\omega^*, \varepsilon)$ represent the neighborhood centered around an exact natural frequency ω^* with the radius equal to the absolute error ε :

$$E(\omega^*, \varepsilon) = [\omega^* - \varepsilon, \omega^* + \varepsilon] \tag{18}$$

This exact natural frequency ω^* is also the exact zero of the infinitely differentiable function $\Delta(\omega)$. According to Lagrange’s mean value theorem, for any approximation $\bar{\omega} \in E(\omega^*, \varepsilon)$, there exists $\eta \in E(\omega^*, |\bar{\omega} - \omega^*|)$, such that

$$\Delta(\bar{\omega}) = \Delta(\omega^*) + \Delta'(\eta)(\bar{\omega} - \omega^*) = \Delta'(\eta)(\bar{\omega} - \omega^*) \tag{19}$$

Thereby,

$$|\Delta(\bar{\omega})| = |\Delta'(\eta)| |\bar{\omega} - \omega^*| \leq M\varepsilon \tag{20}$$

where

$$M = \max_{\eta \in E(\omega^*, |\bar{\omega} - \omega^*|)} |\Delta'(\eta)| \tag{21}$$

This formula shows that the upper bound of $\bar{\omega}$ for identifying the even multiple natural frequencies can be determined if the maximum of $|\Delta'(\omega)|$ is determined for all $\omega \in E(\omega^*, |\bar{\omega} - \omega^*|)$. Generally, as the absolute error ε is a higher-order small quantity with respect to $\omega > 0$, $\Delta'(\omega)$ exhibits monotonic behaviors as long as ε is sufficiently small, which is illustrated in Figure 4.

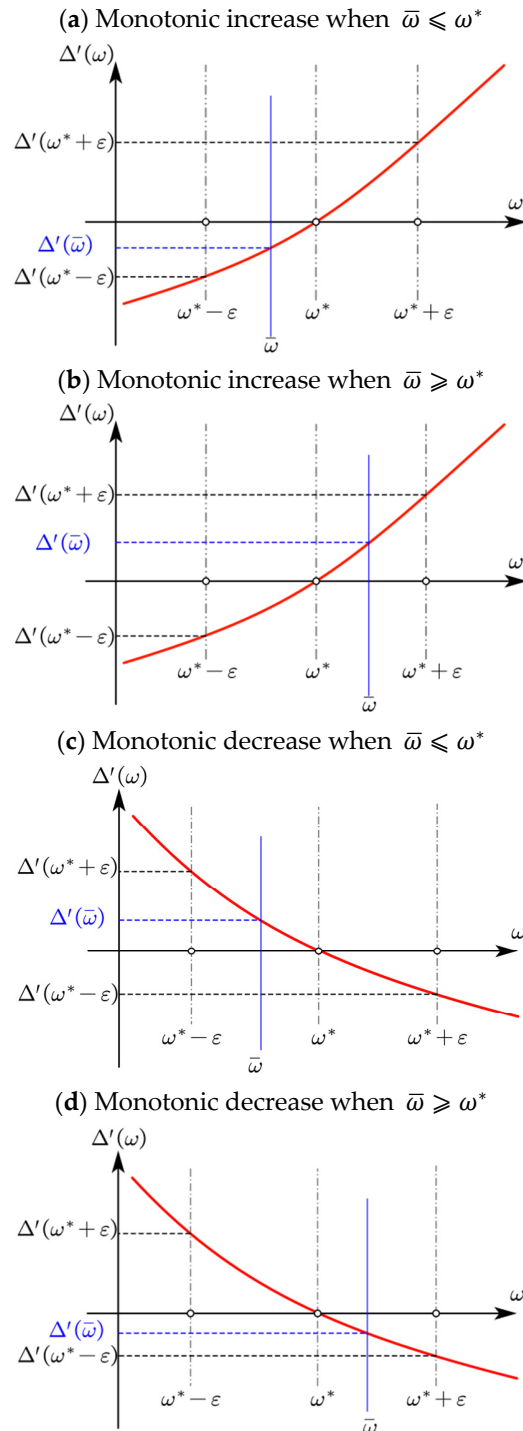


Figure 4. Schematic diagrams of the monotonicity of $\Delta'(\omega)$ near the even multiple natural frequency ω^* (where the red line represent the values of $\Delta'(\omega)$).

Figure 4a,b illustrate the monotonic increase behavior, revealing that $M = -\Delta'(\bar{\omega})$ and $M = \Delta'(\bar{\omega})$ when $\bar{\omega} \leq \omega^*$ and $\bar{\omega} \geq \omega^*$, respectively, while Figure 4c,d illustrate the

monotonic decrease behavior, revealing that $M = \Delta'(\bar{\omega})$ and $M = -\Delta'(\bar{\omega})$ when $\bar{\omega} \leq \omega^*$ and $\bar{\omega} \geq \omega^*$, respectively. Meanwhile, these monotonic behaviors of $\Delta'(\omega)$ near the even multiple natural frequency ω^* can be strictly proved according to Taylor’s mean value theorem, which is presented in Appendix A.

Therefore, the maximum of $|\Delta'(\omega)|$ in the neighborhood $E(\omega^*, |\bar{\omega} - \omega^*|)$ can be obtained as follows:

$$\max_{\eta \in [\min\{\bar{\omega}, \omega^*\}, \max\{\bar{\omega}, \omega^*\}]} |\Delta'(\eta)| = |\Delta'(\bar{\omega})| \tag{22}$$

Then, Equations (20) and (23) yield an estimation for the upper bounds:

$$|\Delta(\bar{\omega})| \leq |\Delta'(\bar{\omega})|\varepsilon \tag{23}$$

This estimation can be intuitively illustrated in Figure 5, where the purple dashed line passing through the point $(\bar{\omega}, \Delta(\bar{\omega}))$ is the tangent of the red curves for $\Delta(\omega)$. Meanwhile, the orange dash-dotted line passing through the point $(\omega^*, 0)$ is parallel to the purple dashed line. It is clear that the numerically obtained even multiple natural frequency $\bar{\omega}$ will satisfy Equation (23) if the absolute error ε is sufficiently small. Figure 5a–d show the variations in $\Delta(\omega)$ corresponding to the monotonic behavior as depicted in Figure 4a–d, where estimations for the upper bounds are marked with gray points. Moreover, the variations in the $\Delta(\omega)$ depicted in Figure 4a–d also correspond to those depicted in Figure 3e, Figure 3a–c, Figure 3d,f, respectively.

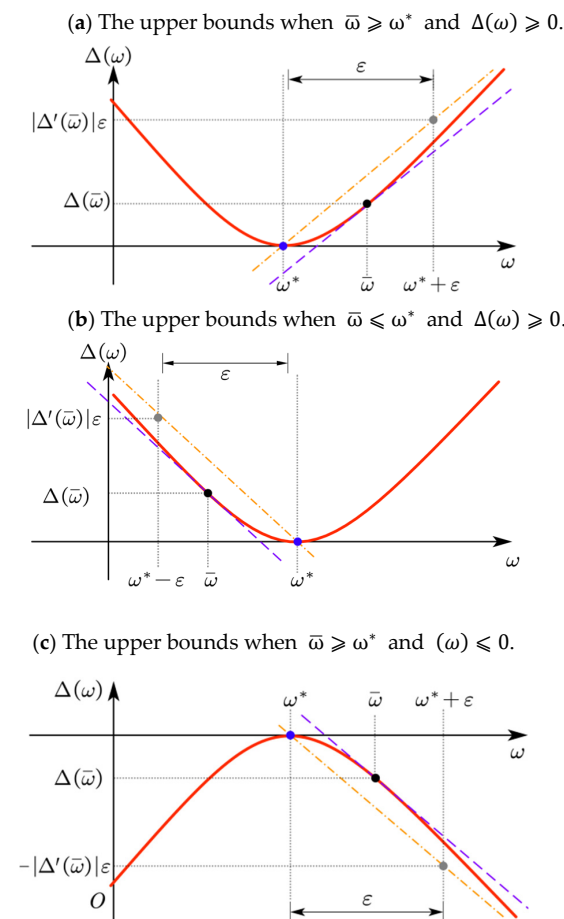


Figure 5. Cont.

(d) The upper bounds when $\bar{\omega} \leq \omega^*$ and $(\omega) \leq 0$.

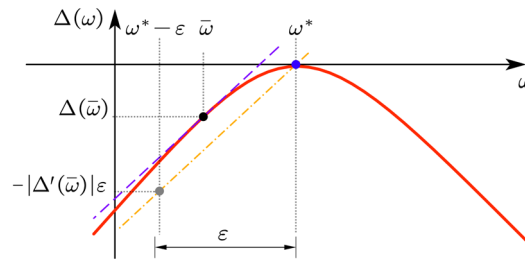


Figure 5. Schematic diagrams illustrating the upper bounds near the even multiple natural frequencies (where the red and thick lines represent the values of the characteristic determinat, the dashed lines represent the tangent lines, and the dash-dotted lines represent the paralell lines of the tangent lines).

Considering the computational rounding error of computers, the numerically computed upper bounds may be lower due to the insufficient precision digits, so a safety factor α is introduced to adjust the estimation for the upper bound. Then, Equation (23) can be further modified to obtain Equation (24):

$$|\Delta(\bar{\omega})| \leq \alpha |\Delta'(\bar{\omega})| \varepsilon \tag{24}$$

It should be noted that the judgment criterion, as shown in Equation (24), also constitutes a theoretically sufficient condition when the absolute error is sufficiently small, which has been proven in Appendix B. Equation (24) also implies that $|\Delta(\bar{\omega})| \rightarrow 0$ if $\varepsilon \rightarrow 0$. Therefore, a zero of Equation (11) is considered as an even multiple natural frequency if Equation (24) is satisfied. For functions that change sharply, the influence of the round-off error will be slightly greater: $\alpha = 1.5 \sim 2$ is recommended.

Subsequently, for the structural system depicted in Figure 1, the judgment criteria specified in Equation (24) can effectively exclude the non-zeros of $\Delta(\omega)$ from the zeros of $\Delta'(\omega)$, which are marked by “○” in Figure 2; therefore, the even multiple natural frequencies are effectively picked out and marked by “△”.

3.4. Determine the Multiplicity of the Natural Frequencies

Based on the equivalent definition for multiple natural frequencies as stated in Equation (10), the multiplicity of a zero of $\Delta(\omega)$ can be theoretically determined by assessing whether it is a zero of its higher-order derivatives. Therefore, the multiplicity of a zero can be determined based on the sign changes in the higher-order derivatives of $\Delta(\omega)$ at two sides of the interval that encompass this zero.

Let ω_{Even}^* and ω_{Odd}^* , respectively, denote the $2m$ multiple and $2m - 1$ multiple natural frequencies, i.e., the $2m$ multiple and $2m - 1$ multiple zeros of the infinitely differentiable function $\Delta(\omega)$, where m is a positive integer. Equation (10) implies that ω_{Even}^* is an odd multiple zero of $\Delta^{(2k-1)}(\omega), k = 1, 2, \dots, m$ but not a zero of $\Delta^{(2m+1)}(\omega)$, and ω_{Odd}^* is an odd multiple zero of $\Delta^{(2k-2)}(\omega), k = 1, 2, \dots, m$ but not a zero of $\Delta^{(2m)}(\omega)$.

Therefore, if the absolute error ε is sufficiently small, then $\Delta^{(2m+1)}(\omega)$ in the domain $E(\omega_{\text{Even}}^*, \varepsilon)$ and $\Delta^{(2m)}(\omega)$ in the domain $E(\omega_{\text{Odd}}^*, \varepsilon)$ exhibit positivity or negativity. This means that the multiplicity of each zero can be determined by observing the sign changes in the derivatives at two sides of the respective intervals surrounding the zeros; i.e., the following conditions should be satisfied:

$$\begin{cases} \Delta^{(2k+1)}(\omega_{\text{Even}}^* + \varepsilon)\Delta^{(2k+1)}(\omega_{\text{Even}}^* - \varepsilon) < 0, k = 0, 1, 2, \dots, m - 1 \\ \Delta^{(2m+1)}(\omega_{\text{Even}}^* + \varepsilon)\Delta^{(2m+1)}(\omega_{\text{Even}}^* - \varepsilon) > 0 \end{cases} \tag{25}$$

for $2m$ multiple natural frequencies and

$$\begin{cases} \Delta^{(2k)}(\omega_{\text{Odd}}^* + \varepsilon)\Delta^{(2k)}(\omega_{\text{Odd}}^* - \varepsilon) < 0, k = 0, 1, 2, \dots, m - 1 \\ \Delta^{(2m)}(\omega_{\text{Odd}}^* + \varepsilon)\Delta^{(2m)}(\omega_{\text{Odd}}^* - \varepsilon) > 0 \end{cases} \quad (26)$$

for $2m - 1$ multiple natural frequencies, respectively. It should be noted that m in the above two equations does not denote the same value. In Equation (25), $2m$ only means a certain even multiple natural frequency with the multiplicity $2m$. In Equation (26), $2m - 1$ means an odd multiple natural frequency with the multiplicity $2m - 1$.

Consider the round-off error in the numerical computation; the above conditions are used to determine the multiplicity and can be adjusted by a safety factor β , typically taken as 1~2 to slightly enlarge the regions $E(\omega_{\text{Even}}^*, \varepsilon)$ and $E(\omega_{\text{Odd}}^*, \varepsilon)$. Thus, based on the preceding discussions, the procedure for determining the multiplicities of natural frequencies utilizing the determinant derivatives is depicted in Figure 6.

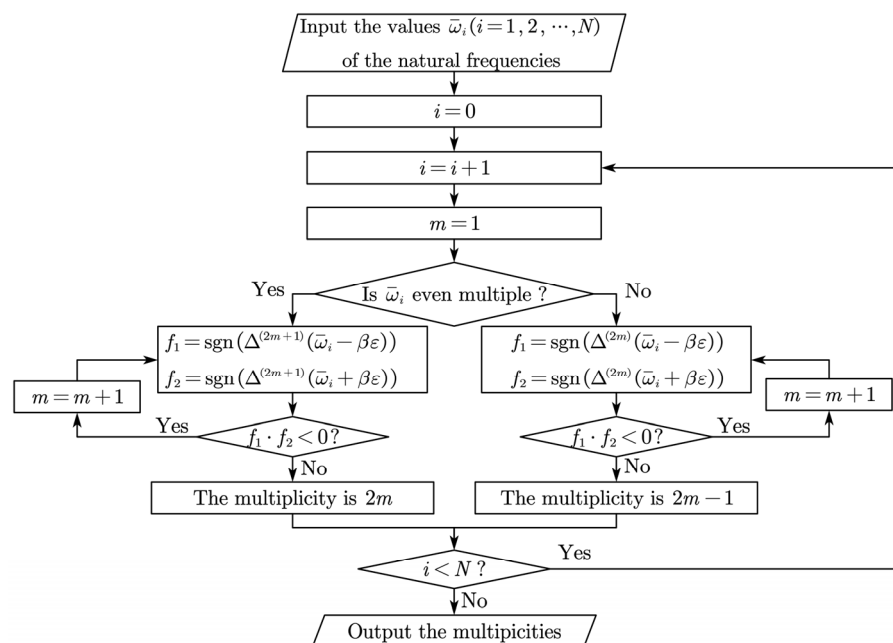


Figure 6. Flowchart of the proposed method for determining the frequency multiplicities.

In Figure 6, N denotes the total number of natural frequency values, with each multiple natural frequency being counted once according to its value. For example, if a system has only two sets of multiple natural frequencies, then N is equal to 2. Take the cantilever beam shown in Figure 1 as a case study to explain in detail the calculation process shown in Figure 6. There should be nine numerically distinct solutions within the frequency range of 20,000 rad/s, i.e., $N = 9$. For these solutions, some of them are obtained by solving Equation (8) with the bisection method, which are considered as odd multiple roots, i.e., odd multiple natural frequencies. Then, the processes on the right branch in Figure 6 can be executed to determine their odd multiplicities. The other part of the solution is obtained by solving (11) using the bisection method and filtering through criterion (24). This part pertains to even multiple roots, i.e., even multiple natural frequencies, so the processes on the left branch in Figure 6 can be executed to obtain their even multiplicities.

Clearly, this procedure necessitates the higher-order derivatives of the characteristic determinant. In view of this, a differentiation formula for computing these derivatives is developed by differentiating the first derivative, i.e., Equation (16), $p - 1$ times, i.e.:

$$\Delta^{(p)}(\omega) = \sum_{k_1=1}^N \sum_{k_2=1}^N \dots \sum_{k_p=1}^N \det \mathbf{U}^{-[k_1, k_2, \dots, k_p]} \quad (27)$$

where each column of matrix $\mathbf{U}^{-[k_1, k_2, \dots, k_p]}$ is defined as

$$\text{col}_j \mathbf{U}^{-[k_1, k_2, \dots, k_p]} = \text{col}_j \mathbf{U}^{-r}(\omega), r = \sum_{m=1}^p s\{j = k_m\} \tag{28}$$

and the function $s\{\cdot\}$ is defined as

$$s\{cond\} = \begin{cases} 1 & \text{if } cond \text{ is true} \\ 0 & \text{if } cond \text{ is false} \end{cases} \tag{29}$$

Thereby, the higher-order derivatives of the determinant can be derived by the derivatives of the coefficient matrix $\bar{\mathbf{U}}$.

3.5. Flowchart of the Proposed Method for Multiple Natural Frequency Analysis

Up to this point, we have proposed a novel method for solving the multiple natural frequencies, namely the determinant-differentiation-based method, which utilizes the first and higher-order derivatives of the characteristic determinant. The proposed method mainly involves calculating the even multiple natural frequencies, picking out the even multiple natural frequencies with the judgment criteria, and determining the multiplicities of all the natural frequencies. The three aspects are integrated and summarized in the flowchart presented in Figure 7.

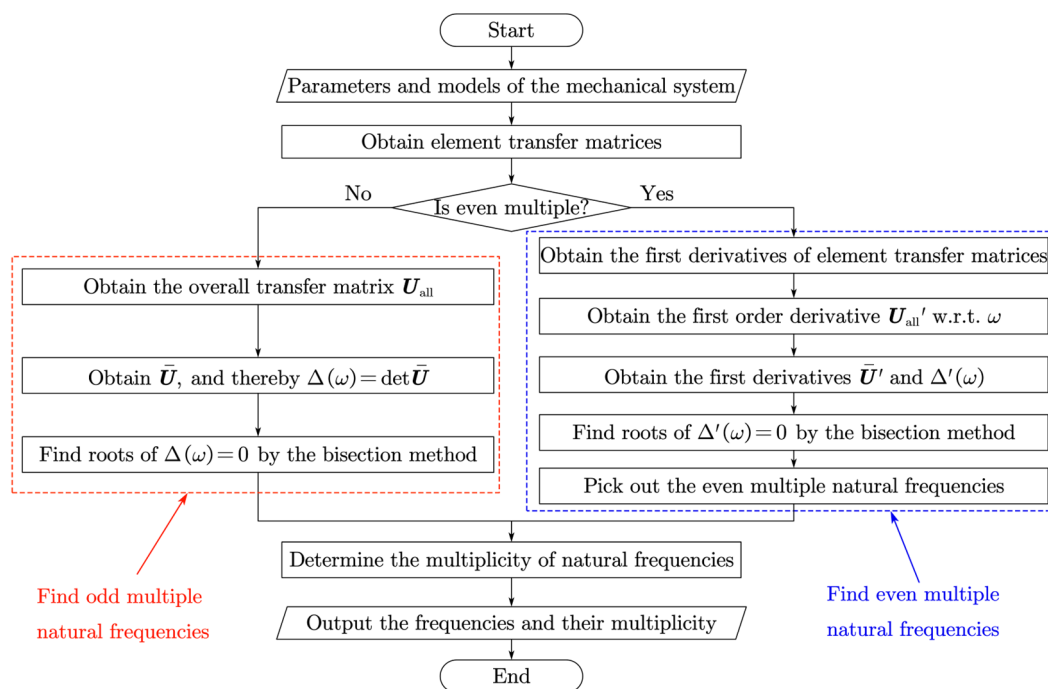


Figure 7. A flowchart illustrating the proposed method for multiple frequency analysis.

In Figure 7, the red box represents the solution method for odd multiple natural frequencies, while the blue box represents the solution method for even multiple natural frequencies. Calculating even multiple natural frequencies with the transfer matrix method requires the computation of the first-order derivative of the element transfer matrices to further obtain the derivative of the overall transfer matrix. There are two steps to obtain the even multiple natural frequencies in the proposed method: (1) find roots of Equation (11) with the bisection method; (2) pick out the natural frequencies among the roots of Equation (11) using the judgment criteria according to Equation (24). The remaining odd multiple natural frequencies, including the distinct natural frequencies, can be directly

obtained by solving Equation (8) using the bisection method. After obtaining the numerical values of all the natural frequencies, the higher-order derivatives are utilized to determine their multiplicities.

4. Numerical Studies

To validate the proposed method for calculating the multiple natural frequencies and determining their multiplicities, several numerical comparative simulations are conducted. The numerical studies include a chain mechanical system, two closed-loop structural systems, and a branch mechanical system. It should be noted that the RESA used in these simulations is conducted with the absolute error, where the sampling process utilizes the linear sampling instead of logarithmic sampling in [39]. Additionally, the original sign-based bisection method in this paper is referred to as the direct bisection method (DBM). All the element transfer matrices used here can be seen in [14]. The safety factors α and β in the proposed method are selected as 1.5 and 1.0, respectively.

4.1. Free Vibration of a Chain Mechanical System with Multiple Natural Frequencies

A spatially vibratory chain mechanical system consisting of four rigid bodies and four springs is illustrated in Figure 8, which exhibits the clamped-free boundary conditions. All the rigid bodies share identical geometric parameters, masses, and moments of inertia. The mass of each rigid body is 1 kg. In the body-fixed frame $x_i y_i z_i$ originating from its input, the mass center and the output of each rigid body are located at $l_{IC,i} = [0.05 \ 0 \ 0]^T$ and $l_{IO,i} = [0.1 \ 0 \ 0]^T$, respectively.

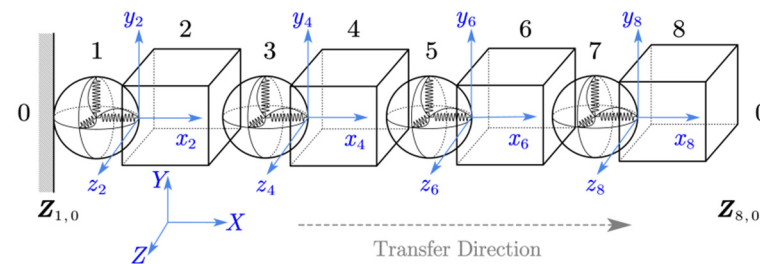


Figure 8. Schematic diagram of spatial chain mechanical system composed of 8 elements numbered from 1 to 8 and with multiple natural frequencies.

If all the geometrical parameters of rigid bodies and spring stiffness are the same in two transverse directions, this system may have even multiple natural frequencies. The moment of inertia projected in the fixed body frame is as follows:

$$J_{i,I} = \begin{bmatrix} 0.001666 & 0 & 0 \\ 0 & 0.0041667 & 0 \\ 0 & 0 & 0.0041667 \end{bmatrix} \text{kg}\cdot\text{m}^2, i = 2, 4, 6, 8 \quad (30)$$

The translational stiffness and torsional stiffness of each spring are identical. The translational stiffness in three directions is $K_x = K_y = K_z = 10^5 \text{ N/m}$, and the torsional stiffness around three axes of the fixed body frame is $K_x' = K_y' = K_z' = 10^3 \text{ N}\cdot\text{m/rad}$.

For this chain mechanical system, the boundary state vector Z_{all} and overall transfer matrix U_{all} are shown as follows:

$$Z_{\text{all}} = [Z_{8,0}^T \ Z_{1,0}^T]^T, U_{\text{all}} = [-I \ T_{1-8}] \quad (31)$$

where I denotes the identity matrix with the order of 12×12 , and T_{1-8} is defined as

$$T_{1-8} = U_8 U_7 U_6 U_5 U_4 U_3 U_2 U_1 \quad (32)$$

where U_i denotes the transfer matrix of element i .

Thus, according to system boundary conditions, the characteristic equation is as follows:

$$\Delta(\omega) = \det \mathbf{U} = \det(\text{col}_{7-18} \mathbf{U}_{\text{all}}) = 0 \tag{33}$$

where $\text{col}_{i \sim j}(\cdot)$ denotes the components of (\cdot) from its i -th to j -th columns.

The required first derivative and higher-order derivatives of the characteristic determinant can be obtained by utilizing Equations (16) and (27), respectively.

This discrete system has 24 degrees of freedom (DOFs), giving rise to 24 modes in total. Due to the similarity in both the Y - and Z -direction regarding the structural property and boundary conditions, the frequencies associated with the transverse vibration in the X - Y and X - Z planes may overlap, resulting in a multiplicity of 2. The natural frequencies calculated through the DBM, RESA, analytical solutions, and proposed method are presented in Table 1. The analytical solutions are obtained by utilizing Lagrange’s formulation. The absolute computing error of 0.01 rad/s is employed, and both the determinant and its derivative are shown in Figure 9.

Table 1. Natural frequencies of the chain mechanical system (unit: rad/s).

Modal Order	1	2	3	4	5	6	7	8
DBM	-	-	109.824	-	-	269.012	316.231	-
RESA	49.600	-	109.824	209.621	-	269.018	316.228	422.053
Analytical	49.603	49.603	109.825	209.619	209.619	269.015	316.228	422.053
Proposed	49.606	49.606	109.824	209.621	209.621	269.012	316.231	422.051
Modal Order	9	10	11	12	13	14	15	16
DBM	-	484.488	-	-	594.316	-	-	774.598
RESA	-	484.492	572.895	-	594.316	754.483	-	774.598
Analytical	422.053	484.489	572.896	572.896	594.314	754.482	754.482	774.597
Proposed	422.051	484.488	572.895	572.895	594.316	754.481	754.481	774.598
Modal Order	17	18	19	20	21	22	23	24
DBM	-	-	1186.754	-	-	1455.762	-	-
RESA	1004.114	-	1186.749	1279.005	-	1455.769	1477.811	-
Analytical	1004.115	1004.115	1186.751	1279.005	1279.005	1455.766	1477.808	1477.808
Proposed	1004.113	1004.113	1186.754	1279.004	1279.004	1455.762	1477.809	1477.809

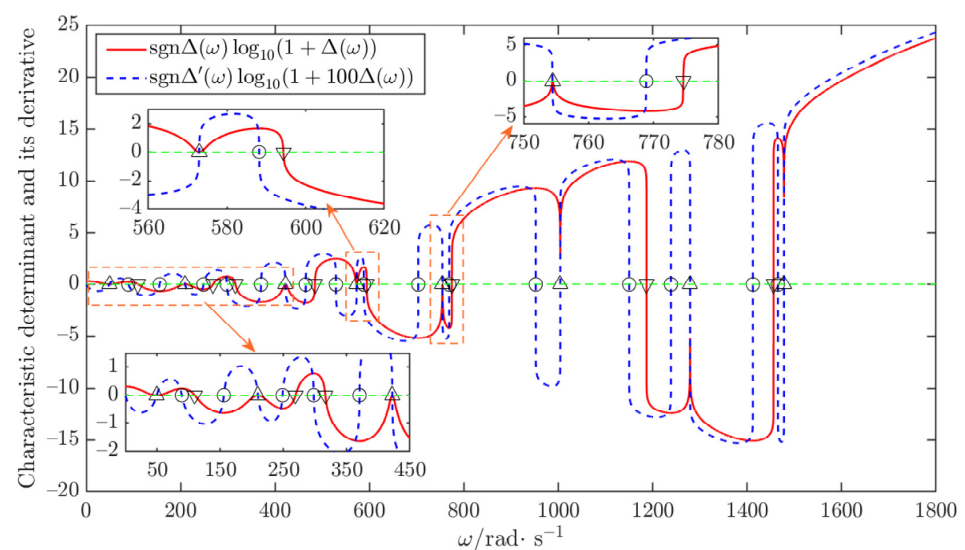


Figure 9. The characteristic determinant and its first derivative of the chain mechanical system (“○”, “▽”, and “△” denote the zeros of the first derivative but not the natural frequencies, the odd multiple natural frequencies, and the even multiple natural frequencies, respectively).

In Figure 9, it can be seen that $\Delta(\omega)$ has eight even multiple zeros and eight odd multiple zeros without counting their multiplicities. This means that this chain system has eight even multiple and eight odd multiple natural frequencies. Consequently, the results presented in Table 1 reveal that this system has eight sets of double natural frequencies and eight distinct natural frequencies. Compared to the analytical solutions, the even multiple natural frequencies cannot be resolved using the DBM. The RESA can only determine numerical values of the natural frequencies without determining their multiplicities. In contrast, the proposed method can effectively resolve the multiple natural frequencies and determine their respective multiplicities. Moreover, Figure 9 demonstrates that the even multiple zeros of the characteristic determinant are also the odd multiple zeros of its first derivative, and the monotonicity of the first derivative of characteristic determinant near the even multiple natural frequencies is consistent with Figure 4 in this simulation.

4.2. Free Vibration of a Closed-Loop Structural System with Multiple Natural Frequencies

A closed-loop structural system composed of four identical square planar rigid bodies and four identical springs is shown in Figure 10, which is vibrating in plane. Each rigid body has a mass of 1 kg, with its center of mass located at its geometric center. The connection point of each rigid body is positioned at the midpoint of the corresponding side. The moment of inertia with respect to the midpoint of any side is $5/12 \text{ kg}\cdot\text{m}^2$. The translational stiffness of each spring is 1000 N/m in the x and y principal directions, and the torsional stiffness is $100 \text{ N}\cdot\text{m/rad}$.

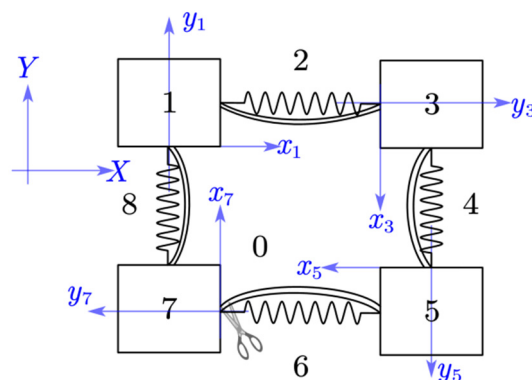


Figure 10. Schematic diagram of a closed-loop mechanical system composed of 8 elements numbered from 1 to 8 and with multiple natural frequencies.

If all the rigid bodies and springs are the same, this system may have multiple natural frequencies. These elements form a transfer closed loop. Therefore, in MSTMM, the system overall transfer matrix can be obtained as follows:

$$U_{\text{all}} = T_{1-8} - I, T_{1-n} = U_8 \cdots U_2 U_1 \tag{34}$$

where $U_j (j = 1, 2, \dots, 8)$ denotes the transfer matrix of element j . For the closed-loop system, the coefficient matrix \bar{U} of the eigen-equation is equal to U_{all} .

This system has 12 DOFs, resulting in 12 vibration modes. The first three natural frequencies correspond to zero values and represent the free displacement modes. Frequencies obtained through the DBM, RESA, analytical solutions, and the proposed method in this paper are presented in Table 2, where the first three zero frequencies are excluded, and the absolute error is set to 0.001 rad/s .

Table 2. Frequencies of the closed-loop system composed of rigid bodies and springs (unit: rad/s).

Modal Order	4	5	6	7	8	9	10	11	12
DBM	-	-	44.721	-	-	48.990	-	-	89.443
RESA	40.601	-	44.721	-	-	-	80.942	-	89.443
Analytical	40.601	40.601	44.721	44.721	44.721	48.990	80.942	80.942	89.443
Proposed	40.602	40.602	44.721	44.721	44.721	48.990	80.942	80.942	89.443

The results show that, after excluding the free displacement modes, this system has two sets of double natural frequencies, one set of triple natural frequencies and two distinct natural frequencies, resulting in nine non-zero natural frequencies in total. Meanwhile, it is evident that the DBM can neither resolve the even multiple natural frequencies of the system nor determine the multiplicities of all frequencies. The RESA cannot determine the frequency multiplicities, and the 9-th natural frequency is missed when the sample number is set to 100. The proposed method in this paper obtains all the multiple natural frequencies and correctly gives their multiplicities. The curves corresponding to the characteristic determinant and its first two derivatives are plotted in Figure 11.

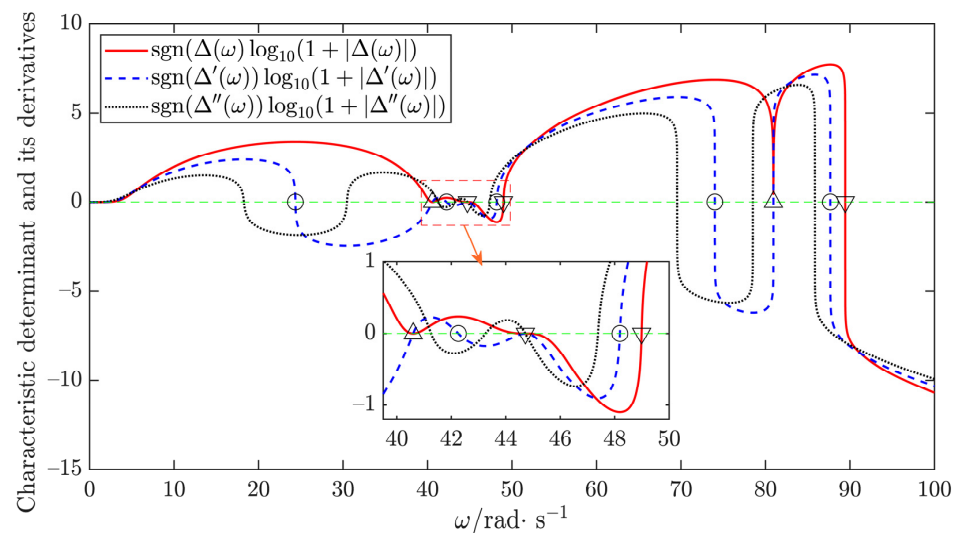


Figure 11. Characteristic determinant and the first two derivatives of the closed system (“○”, “▽”, and “△” denote the zeros of the first derivative but not the natural frequencies, odd multiple natural frequencies, and even multiple natural frequencies, respectively).

In Figure 11, it can be observed that three curves pass through the horizontal axes and intersect at the same point within the range of 44 rad/s to 46 rad/s, indicating the presence of a natural frequency with a multiplicity of at least 3. Through our calculations, we identified a solution at 44.721 rad/s, which satisfies cases $k = 1$ and 2 in Equation (26), but not $k = 3$. Therefore, this solution can be identified as a triple natural frequency as presented in Table 2. Moreover, the monotonicity of the first derivative of the characteristic determinant near the double natural frequencies is also consistent with the descriptions illustrated in Figure 4; thus, the criteria are feasible for picking out these even multiple natural frequencies among the zeros of $\Delta'(\omega)$.

4.3. Free Vibration of a Regular Hexagonal Structure with Multiple Natural Frequencies

A regular hexagonal structure vibrating in plane is illustrated in Figure 12. This structure consists of six straight uniform Euler beams with circular cross-sections, which consider the axial tension. The beams are connected end to end by six nodes, with each node containing spring supports in two principal directions. In this configuration, the

beams and supported nodes are marked by odd numbers from 1 to 11 and even numbers from 2 to 12, respectively.

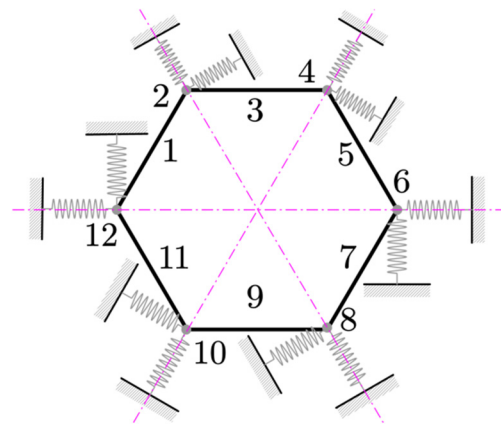


Figure 12. Schematic diagram of a regular hexagonal structure composed of 12 elements numbered from 1 to 12 and with multiple natural frequencies.

The system can be considered as a closed-loop system consisting of six rigid bodies and six supports; that is, these twelve elements form a transfer loop. If all beams and supports are the same except for their orientations, the system will exhibit multiple natural frequencies. Here, the Young’s modulus of the Euler beam is 200 GPa, the section radius is 0.025 m, the density is 7800 kg/m³, and the length is 1 m. The boundary bearing stiffness in both principal directions is 1000 N/m. Therefore, this structure can be regarded as a closed-loop system. The overall transfer matrix follows the same form as Equation (34), i.e.:

$$\mathbf{U}_{\text{all}} = \mathbf{T}_{1-12} - \mathbf{I}, \mathbf{T}_{1-12} = \mathbf{U}_{12} \cdots \mathbf{U}_2 \mathbf{U}_1 \tag{35}$$

where the matrices $\mathbf{U}_1, \mathbf{U}_3, \dots, \mathbf{U}_{11}$ denote the transfer matrix of the Euler beams numbered as 1, 3, ..., 11 while the matrices $\mathbf{U}_2, \mathbf{U}_4, \dots, \mathbf{U}_{12}$ denote the transfer matrix of the spring supports numbered as 2, 4, ..., 12. The coefficient matrix $\bar{\mathbf{U}}$ of the eigen-equation is also equal to \mathbf{U}_{all} in this simulation.

The natural frequencies obtained using the DBM, RESA, FEM, and proposed method in this paper are presented in Table 3, where the absolute error adopted in the DBM, RESA, and proposed method is 0.01 rad/s. The FEM is used to provide the reference results by dividing each Euler beam into 20 two-node Euler beam elements considering the tensile DOFs.

Table 3. Natural frequencies of the regular hexagonal structure system (unit: rad/s).

Modal Order	1	2	3	4	5	6	7
DBM	-	-	8.851	-	-	483.359	624.390
RESA	8.081	-	8.852	193.670	-	483.360	624.387
FEM	8.080	8.080	8.852	193.667	193.667	483.359	624.385
Proposed	8.084	8.084	8.851	193.670	193.670	483.359	624.390

The results show there are two pairs of double natural frequencies and three distinct natural frequencies in the first seven natural frequencies, revealing that the proposed method can effectively obtain the even and odd multiple natural frequencies as well as their multiplicities, compared with the RESA and DBM.

4.4. Free Vibration of a Branch Mechanical System

A branch system consisting of a planar square rigid body and four planar spring elements, as illustrated in Figure 13, is chosen to validate the proposed method for the

branch mechanical systems. The choice is motivated by the fact that the analytical solutions for this simple system can be directly derived. In this system, each spring connects the midpoint of each side of the rigid body to the system boundary. The square rigid body has a side length of $2a$, mass m , and the moment of inertial $J_z = 5 ma^2/3$ with respect to the midpoint of each side. Each spring has the translational stiffness denoted by $K_{x,i} = K_x, K_{y,i} = K_y (i = 2, 3, 4, 5)$ and angular stiffness denoted by $K'_{z,i} = K_r (i = 2, 3, 4, 5)$.

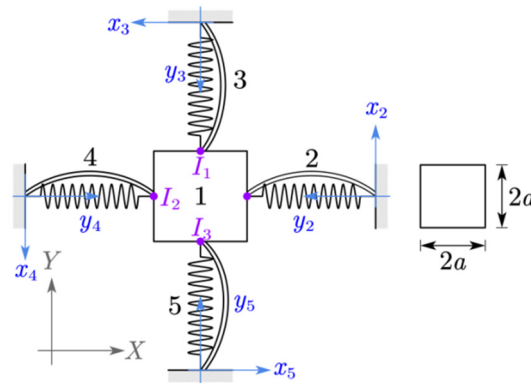


Figure 13. Schematic diagram of a simple branch system composed of 5 elements numbered from 1 to 5 and with multiple natural frequencies.

When parameters are specially chosen, this system will have double natural frequencies or triple natural frequencies. The boundary state vector Z_{all} is chosen as follows:

$$Z_{all} = [Z_{2,0}^T \quad Z_{3,0}^T \quad Z_{4,0}^T \quad Z_{5,0}^T]^T \tag{36}$$

Therefore, the overall transfer matrix can be obtained by the automatic assembly method [14] and expressed as follows:

$$U_{all} = \begin{bmatrix} -I & T_{3-2} & T_{4-2} & T_{5-2} \\ O_{3 \times 6} & G_{3-1} & G_{4-1} & O_{3 \times 6} \\ O_{3 \times 6} & G_{3-1} & O_{3 \times 6} & G_{5-1} \end{bmatrix} \tag{37}$$

$$\begin{cases} T_{3-2} = U_2 U_{1,I_1} U_3, T_{4-2} = U_2 U_{1,I_2} U_4, T_{5-2} = U_2 U_{1,I_3} U_5, \\ G_{3-1} = -H_{1,I_1} U_3, G_{4-1} = H_{1,I_2} U_4, G_{5-1} = H_{1,I_3} U_5 \end{cases} \tag{38}$$

where U_2, U_3, U_4 , and U_5 denote the transfer matrices of the four springs, while U_{1,I_1}, U_{1,I_2} , and U_{1,I_3} denote the transfer matrices of rigid body 1 from its three inputs to output.

According to the system boundary conditions, the coefficient matrix of the eigen-equation expressed in Equation (1) is as follows:

$$\bar{U} = \text{col}_{4-6,10-12,16-18,22-24} U_{all} \tag{39}$$

The natural frequencies of this simple system can be analytically obtained using the following equation:

$$\omega_1 = 2\sqrt{\frac{K_x}{m}}, \omega_2 = 2\sqrt{\frac{K_y}{m}}, \omega_3 = \sqrt{\frac{4K_r + 2(K_x + K_y)a^2}{J_z - ma^2}} \tag{40}$$

Typically, this system has three distinct natural frequencies, marked as Case A. Another two exceptional cases are marked as Case B and Case C, where Case B is defined by supplementing the condition $K_x = K_y = K$ based on Case A, and Case C is defined by supplementing the condition $K_r = K(J_z - 2ma^2)/m$ based on Case B.

For Case B, the system contains one pair of double natural frequencies and a single natural frequency, i.e.,

$$\omega_1 = \omega_2 = 2\sqrt{\frac{K}{m}}, \omega_3 = 2\sqrt{\frac{K_r + a^2K}{J_z - ma^2}} \tag{41}$$

For Case C, the system contains only one set of triple natural frequencies, i.e.,

$$\omega_{1,2,3} = 2\sqrt{\frac{K}{m}} \tag{42}$$

To conduct a numerical study to validate the effectiveness of the proposed method for the branch mechanical systems, the parameters in Case A, B, and C are chosen as follows:

$$\begin{cases} \text{CaseA : } m = 1 \text{ kg, } a = 0.5 \text{ m, } K_r = 10 \text{ N}\cdot\text{m/rad, } K_x = 100 \text{ N/m, } K_y = 200 \text{ N/m;} \\ \text{CaseB : } m = 1 \text{ kg, } a = 0.5 \text{ m, } K_r = 10 \text{ N}\cdot\text{m/rad, } K = 100 \text{ N/m;} \\ \text{CaseC : } m = 1 \text{ kg, } a = 0.5 \text{ m, } K = 100 \text{ N/m} \end{cases} \tag{43}$$

The calculation results are shown in Table 4. Among them, the absolute computational error in the proposed method is taken as 0.001 rad/s, and the numerical values of the analytical solutions can be obtained using Equations (40)–(43).

Table 4. Natural frequencies of the branch mechanical system.

Method Model Order	Analytical (rad·s ⁻¹)			Proposed Method (rad·s ⁻¹)		
	1	2	3	1	2	3
Case A	20.000	28.284	33.764	20.000	28.284	33.764
Case B	20.000	20.000	28.983	20.000	20.000	28.983
Case C	20.000	20.000	20.000	20.000	20.000	20.000

Table 4 reveals that the proposed method can be used to effectively calculate the multiple natural frequencies of this branch system and determine their multiplicities.

5. Conclusions

This paper proposes a novel method, named the determinant-differentiation-based method, for calculating the multiple natural frequencies and their multiplicities. It enables the TMM, as well as MSTMM, to effectively calculate the multiple natural frequencies and determine their multiplicities, where the latter has not been addressed previously pertaining to the MSTMM or TMM. Four comparative simulations show that the calculation accuracy of the proposed method agrees well with the available analytical solutions or the finite element method. The proposed method makes the following contributions:

- (1) By differentiating the characteristic determinant with respect to the natural frequency, the proposed method effectively calculates the even multiple natural frequencies of the mechanical or structural systems. This is achieved by transforming the even multiple natural frequencies into the odd multiple zeros of the first derivative of determinant, and the odd multiple zeros can be directly obtained with the bisection method.
- (2) The proposed judgment criteria can effectively pick out the even multiple natural frequencies among the zeros of the first derivative of the characteristic determinant, in which the upper bounds can adaptively change with the absolute error from the true zeros.
- (3) The higher-order derivatives of the characteristic determinant are derived and utilized to accurately determine the multiplicities of all the natural frequencies.

This paper also provides a method for solving the real nonlinear eigen-problem with multiple eigenvalues and with a middle- or low-rank matrix, including solving their

eigenvalues and multiplicities. In the proposed method, we have taken into account numerical stability and therefore avoided matrix inversion. This guarantees the stability and reliability of the processes of picking out the even natural frequencies from the first derivative of the characteristic determinant and determining their multiplicities. It is worth noting that the differentiability of element transfer matrices may play a crucial role in the overall differentiability of the method. If the element transfer matrices are not differentiable, it could potentially introduce challenges when applying the proposed method. Future research will focus on improving the computational efficiency of the method proposed in this paper, such as enhancing the computational efficiency of the system’s overall transfer matrix, combining it with more efficient iterative procedures, and accurately counting the eigenvalues.

Author Contributions: Conceptualization, J.W. and B.H.; methodology, J.W.; software, K.X.; validation, J.W., X.R. and X.W.; formal analysis, B.H. and J.Z.; original draft preparation, J.W., B.H. and X.W. All authors have read and agreed to the published version of the manuscript.

Funding: This research was funded by the National Science Foundation of China Government (No. 11972193 and No. 92266201).

Data Availability Statement: Data available on request from the authors.

Conflicts of Interest: The authors declare no conflicts of interest.

Appendix A. A Proof for the Monotonicity near the Even Multiple Natural Frequencies

Assume that ω^* is an exact even multiple natural frequency with the multiplicity $2m$, where m is a positive integer; for any real positive number $\omega \in E(\omega^*, \varepsilon)$, there exists a real number $\eta \in E(\omega^*, |\omega - \omega^*|)$, such that

$$\Delta''(\omega) = \frac{1}{(2m - 2)!} \Delta^{(2m)}(\eta)(\omega - \omega^*)^{2m-2} \tag{A1}$$

$\Delta^{(2m)}(\omega^*) \neq 0$ for the infinitely differentiable function $\Delta(\omega)$ near the ω^* because the $2m$ -multiple natural frequencies are also the $2m$ -multiple zeros of $\Delta(\omega)$. Therefore, for any $\delta > 0$, there will exist $\mu > 0$, such that

$$\left| \Delta^{(2m)}(\omega) - \Delta^{(2m)}(\omega^*) \right| < \delta, \forall \omega \in E(\omega^*, \mu) \tag{A2}$$

If $\delta = \left| \Delta^{(2m)}(\omega^*) \right|$, it yields that, for all $\omega \in E(\omega^*, \mu)$,

$$\Delta^{(2m)}(\omega^*) - \delta < \Delta^{(2m)}(\omega) < \Delta^{(2m)}(\omega^*) + \delta \tag{A3}$$

This implies that

$$\begin{cases} \Delta^{(2m)}(\omega) > 0, \text{ if } \Delta^{(2m)}(\omega^*) > 0 \\ \Delta^{(2m)}(\omega) < 0, \text{ if } \Delta^{(2m)}(\omega^*) < 0 \end{cases} \tag{A4}$$

Therefore, for $\Delta^{(2m)}(\omega)$, no zeros exist within $E(\omega^*, \varepsilon)$ if ε is sufficiently small, i.e., $\varepsilon < \mu$, which yields the following:

$$\begin{cases} \Delta''(\omega) > 0, \text{ if } \Delta^{(2m)}(\omega^*) > 0 \\ \Delta''(\omega) < 0, \text{ if } \Delta^{(2m)}(\omega^*) < 0 \end{cases} \tag{A5}$$

Therefore, the monotonicity of $\Delta'(\omega)$ near the even multiple zeros when ε is sufficiently small, which is illustrated as Figure 4, is proved.

Appendix B. A Proof for the Sufficiency of the Judgment Criteria

The sufficiency can be proven via its contrapositive wherein, if $\hat{\omega}^*$ is not the zero of Δ , Equation (24) will be not satisfied even if the absolute error ε is sufficiently small.

For any non-zero $\hat{\omega}^*$ of Δ and absolute error ε , if no zeros exist in the region $E(\hat{\omega}^*, \varepsilon)$, there will certainly be a nonzero minimum of $|\Delta(\omega)|$ with respect to ω in $E(\hat{\omega}^*, \varepsilon)$, which yields the following:

$$\min_{\omega \in E(\hat{\omega}^*, \varepsilon)} |\Delta(\omega)| > 0 \tag{A6}$$

Therefore, for any $\varepsilon_0 < \varepsilon_1 = \min \left\{ \varepsilon, \min_{\omega \in E(\hat{\omega}^*, \varepsilon)} |\Delta(\omega)| / \left(\alpha \max_{\xi \in E(\hat{\omega}^*, \varepsilon)} |\Delta'(\xi)| \right) \right\}$,

Such that

$$\begin{aligned} \min_{\omega \in E(\hat{\omega}^*, \varepsilon_0)} |\Delta(\omega)| &\geq \min_{\omega \in E(\hat{\omega}^*, \varepsilon)} |\Delta(\omega)| \geq \alpha \max_{\xi \in E(\hat{\omega}^*, \varepsilon)} |\Delta'(\xi)| \varepsilon_1 \\ &> \alpha \max_{\xi \in E(\hat{\omega}^*, \varepsilon_0)} |\Delta'(\xi)| \varepsilon_0 \end{aligned} \tag{A7}$$

Therefore, it yields that for all $\omega \in E(\hat{\omega}^*, \varepsilon_0)$,

$$\begin{aligned} |\Delta(\omega)| &\geq \min_{\omega \in E(\hat{\omega}^*, \varepsilon_0)} |\Delta(\omega)| \\ &> \alpha \max_{\xi \in E(\hat{\omega}^*, \varepsilon_0)} |\Delta'(\xi)| \varepsilon_0 \geq \alpha |\Delta'(\omega)| \varepsilon_0 \end{aligned} \tag{A8}$$

Therefore, when ε is sufficiently small, the criterion shown in Equation (24) is also a sufficient condition, i.e., $\hat{\omega}^*$ is the zero of Δ if it is satisfied.

References

- Kopets, E.; Karimov, A.; Scalera, L.; Butusov, D. Estimating natural frequencies of cartesian 3D printer based on kinematic scheme. *Appl. Sci.* **2022**, *12*, 4514. [\[CrossRef\]](#)
- Lu, H.; Rui, X.; Zhang, X. Transfer matrix method for linear vibration analysis of flexible multibody systems. *J. Sound Vib.* **2023**, *549*, 117565. [\[CrossRef\]](#)
- Beck, J.; Brown, J.M.; Scott-Emuakpor, O.E.; Kaszynski, A.; Henry, E.B. Modal expansion method for eigensensitivity calculations of cyclically symmetric bladed disks. *AIAA J.* **2018**, *56*, 4112–4120. [\[CrossRef\]](#)
- Yoon, G.; Donoso, A.; Bellido, J.C.; Ruiz, D. Highly efficient general method for sensitivity analysis of eigenvectors with repeated eigenvalues without passing through adjacent eigenvectors. *Int. J. Numer. Methods Eng.* **2020**, *121*, 4473–4492. [\[CrossRef\]](#)
- Zhang, G.; Khandelwal, K.; Guo, T. Topology optimization of stability-constrained structures with simple/multiple eigenvalues. *Int. J. Numer. Methods Eng.* **2024**, *125*, e7387. [\[CrossRef\]](#)
- Bathe, K.-J. *Finite Element Procedures*, 2nd ed.; Prentice Hall: Hoboken, NJ, USA, 2006; pp. 838–860.
- Iwamoto, H.; Hisano, S.; Tanaka, N. Modelling and feedforward control of wave propagation in an orthotropic rectangular panel based on a transfer matrix method. *J. Sound Vib.* **2020**, *487*, 115639. [\[CrossRef\]](#)
- Ling, M.; Yuan, L.; Zhou, H.; Ning, M. Modified transfer matrix method for vibration analysis of beam structures including branches and rigid bodies. *Mech. Syst. Signal Process.* **2023**, *187*, 109858. [\[CrossRef\]](#)
- Lund, J.W. Stability and damped critical speeds of a flexible rotor in fluid-film bearings. *J. Eng. Ind.* **1974**, *96*, 509–517. [\[CrossRef\]](#)
- Luo, Z.; Bian, Z.; Zhu, Y.; Liu, H. An improved transfer-matrix method on steady-state response analysis of the complex rotor-bearing system. *Nonlinear Dyn.* **2020**, *102*, 101–113. [\[CrossRef\]](#)
- Hsieh, S.-C.; Chen, J.-H.; Lee, A.-C. A modified transfer matrix method for the coupled lateral and torsional vibrations of asymmetric rotor-bearing systems. *J. Sound Vib.* **2008**, *312*, 563–571. [\[CrossRef\]](#)
- Cao, Y.; Liu, G.; Hu, Z. Vibration calculation of pipeline systems with arbitrary branches by the hybrid energy transfer matrix method. *Thin-Walled Struct.* **2023**, *183*, 110442. [\[CrossRef\]](#)
- Dell, A.; Krynkina, A.; Horoshenkov, K.V. The use of the transfer matrix method to predict the effective fluid properties of acoustical systems. *Appl. Acoust.* **2021**, *182*, 108259. [\[CrossRef\]](#)
- Rui, X.; Wang, G.; Zhang, J. *Transfer Matrix Method for Multibody Systems: Theory and Applications*; John Wiley & Sons: Hoboken, NJ, USA, 2018.
- Rui, X.; Zhang, J.; Wang, X.; Rong, B.; He, B.; Jin, Z. Multibody system transfer matrix method: The past, the present, and the future. *Int. J. Mech. Syst. Dyn.* **2022**, *2*, 3–26. [\[CrossRef\]](#)
- Wang, X.; Xia, P. Novel modeling and vibration analysis method on a helicopter drive train system. *AIAA J.* **2022**, *60*, 4288–4301. [\[CrossRef\]](#)

17. Chen, D.; Gu, C.; Marzocca, P.; Yang, J.; Pan, G. Dynamic modeling of rotating blades system based on transfer matrix method of multibody system. *Appl. Math. Model.* **2022**, *105*, 475–495. [[CrossRef](#)]
18. Mehrmann, V.; Voss, H. Nonlinear eigenvalue problems: A challenge for modern eigenvalue methods. *GAMM-Mitteilungen* **2004**, *27*, 121–152. [[CrossRef](#)]
19. Zhang, X. *Matrix Analysis and Applications*; Cambridge University Press: London, UK, 2017.
20. Ruhe, A. Algorithms for the nonlinear eigenvalue problem. *SIAM J. Numer. Anal.* **1973**, *10*, 674–689. [[CrossRef](#)]
21. Yang, C.; Hua, D. The quadratic approximation methods for solving nonlinear eigenvalue problems. *Math. Numer. Sin.* **2014**, *36*, 381–392. [[CrossRef](#)]
22. Chen, X.-P.; Wei, W.; Pan, X.-M. Modified successive approximation methods for the nonlinear eigenvalue problems. *Appl. Numer. Math.* **2021**, *164*, 190–198. [[CrossRef](#)]
23. Chen, X.; Dai, H.; Wei, W. Successive mth approximation method for the nonlinear eigenvalue problem. *Comput. Appl. Math.* **2017**, *36*, 1009–1021. [[CrossRef](#)]
24. Van Beeumen, R.; Meerbergen, K.; Michiels, W. A Rational Krylov Method Based on Hermite Interpolation for Nonlinear Eigenvalue Problems. *SIAM J. Sci. Comput.* **2013**, *35*, A327–A350. [[CrossRef](#)]
25. Voss, H. A Jacobi–Davidson method for nonlinear and nonsymmetric eigenproblems. *Comput. Struct.* **2007**, *85*, 1284–1292. [[CrossRef](#)]
26. Zheng, C.J.; Zhang, C.; Bi, C.X.; Gao, H.F.; Du, L.; Chen, H.B. Coupled FE–BE method for eigenvalue analysis of elastic structures submerged in an infinite fluid domain. *Int. J. Numer. Methods Eng.* **2017**, *110*, 163–185. [[CrossRef](#)]
27. Baydoun, S.K.; Voigt, M.; Goderbauer, B.; Jelic, C.; Marburg, S. A subspace iteration eigensolver based on Cauchy integrals for vibroacoustic problems in unbounded domains. *Int. J. Numer. Methods Eng.* **2021**, *122*, 4250–4269. [[CrossRef](#)]
28. Wittrick, W.H.; Williams, F.W. A general algorithm for computing natural frequencies of elastic structures. *Q. J. Mech. Appl. Math.* **1971**, *24*, 263–284. [[CrossRef](#)]
29. Williams, F.W.; Yuan, S.; Ye, K.; Kennedy, D.; Djoudi, M.S. Towards deep and simple understanding of the transcendental eigenproblem of structural vibrations. *J. Sound Vib.* **2002**, *256*, 681–693. [[CrossRef](#)]
30. Sun, X. The application of the Wittrick-Williams algorithm for free vibration analysis of cracked skeletal structures. *Thin-Walled Struct.* **2020**, *159*, 107307. [[CrossRef](#)]
31. Papkov, S.O.; Banerjee, J.R. Dynamic stiffness formulation and free vibration analysis of specially orthotropic Mindlin plates with arbitrary boundary conditions. *J. Sound Vib.* **2019**, *458*, 522–543. [[CrossRef](#)]
32. Han, F.; Dan, D.; Cheng, W. Extension of dynamic stiffness method to complicated damped structures. *Comput. Struct.* **2018**, *208*, 143–150. [[CrossRef](#)]
33. Han, F.; Dan, D.; Cheng, W.; Jubao, Z. An improved Wittrick-Williams algorithm for beam-type structures. *Compos. Struct.* **2018**, *204*, 560–566. [[CrossRef](#)]
34. Carrera, E.; Pagani, A.; Banerjee, J.R. Linearized buckling analysis of isotropic and composite beam-columns by Carrera Unified Formulation and dynamic stiffness method. *Mech. Adv. Mater. Struct.* **2016**, *23*, 1092–1103. [[CrossRef](#)]
35. Náprstek, J.; Fischer, C. Investigation of bar system modal characteristics using Dynamic Stiffness Matrix polynomial approximations. *Comput. Struct.* **2017**, *180*, 3–12. [[CrossRef](#)]
36. Yuan, S.; Ye, K.; Williams, F.W.; Kennedy, D. Recursive second order convergence method for natural frequencies and modes when using dynamic stiffness matrices. *Int. J. Numer. Methods Eng.* **2003**, *56*, 1795–1814. [[CrossRef](#)]
37. Murthy, D.V. Solution and sensitivity analysis of a complex transcendental eigenproblem with pairs of real eigenvalues. *Int. J. Numer. Methods Eng.* **1992**, *33*, 115–129. [[CrossRef](#)]
38. Huiyn, X. A combined dynamic finite element—Riccati transfer matrix method for solving non-linear eigenproblems of vibrations. *Comput. Struct.* **1994**, *53*, 1257–1261. [[CrossRef](#)]
39. Bestle, D.; Abbas, L.; Rui, X. Recursive eigenvalue search algorithm for transfer matrix method of linear flexible multibody systems. *Multibody Syst. Dyn.* **2014**, *32*, 429–444. [[CrossRef](#)]
40. Quarteroni, A.; Sacco, R.; Saleri, F. *Numerical Mathematics*, 2nd ed.; Springer: Berlin/Heidelberg, Germany, 2007.
41. Ypma, T.J. Finding a Multiple Zero by Transformations and Newton-Like Methods. *SIAM Rev.* **1983**, *25*, 365–378. [[CrossRef](#)]

Disclaimer/Publisher’s Note: The statements, opinions and data contained in all publications are solely those of the individual author(s) and contributor(s) and not of MDPI and/or the editor(s). MDPI and/or the editor(s) disclaim responsibility for any injury to people or property resulting from any ideas, methods, instructions or products referred to in the content.